



Acid Experimental Evolution of the Haloarchaeon *Halobacterium* sp. NRC-1 Selects Mutations Affecting Arginine Transport and Catabolism

Karina S. Kunka^{1,2}, Jessie M. Griffith^{1,2}, Chase Holdener¹, Katarina M. Bischof¹, Haofan Li¹, Priya DasSarma², Shiladitya DasSarma² and Joan L. Slonczewski^{1*}

¹ Department of Biology, Kenyon College, Gambier, OH, United States, ² Institute of Marine and Environmental Technology, Department of Microbiology and Immunology, University of Maryland School of Medicine, Baltimore, MD, United States

OPEN ACCESS

Edited by:

Francisco Rodríguez-Valera,
Universidad Miguel Hernández
de Elche, Spain

Reviewed by:

Zhenfeng Zhang,
Institute of Microbiology (CAS), China
Miyako Shiraishi,
Osaka University, Japan

*Correspondence:

Joan L. Slonczewski
slonczewski@kenyon.edu

Specialty section:

This article was submitted to
Biology of Archaea,
a section of the journal
Frontiers in Microbiology

Received: 22 December 2019

Accepted: 12 March 2020

Published: 24 April 2020

Citation:

Kunka KS, Griffith JM, Holdener C, Bischof KM, Li H, DasSarma P, DasSarma S and Slonczewski JL (2020) Acid Experimental Evolution of the Haloarchaeon *Halobacterium* sp. NRC-1 Selects Mutations Affecting Arginine Transport and Catabolism. *Front. Microbiol.* 11:535. doi: 10.3389/fmicb.2020.00535

Halobacterium sp. NRC-1 (NRC-1) is an extremely halophilic archaeon that is adapted to multiple stressors such as UV, ionizing radiation and arsenic exposure; it is considered a model organism for the feasibility of microbial life in iron-rich brine on Mars. We conducted experimental evolution of NRC-1 under acid and iron stress. NRC-1 was serially cultured in CM⁺ medium modified by four conditions: optimal pH (pH 7.5), acid stress (pH 6.3), iron amendment (600 μM ferrous sulfate, pH 7.5), and acid plus iron (pH 6.3, with 600 μM ferrous sulfate). For each condition, four independent lineages of evolving populations were propagated. After 500 generations, 16 clones were isolated for phenotypic characterization and genomic sequencing. Genome sequences of all 16 clones revealed 378 mutations, of which 90% were haloarchaeal insertion sequences (ISH) and ISH-mediated large deletions. This proportion of ISH events in NRC-1 was five-fold greater than that reported for comparable evolution of *Escherichia coli*. One acid-evolved clone had increased fitness compared to the ancestral strain when cultured at low pH. Seven of eight acid-evolved clones had a mutation within or upstream of *arcD*, which encodes an arginine-ornithine antiporter; no non-acid adapted strains had *arcD* mutations. Mutations also affected the *arcR* regulator of arginine catabolism, which protects bacteria from acid stress by release of ammonia. Two acid-adapted strains shared a common mutation in *bop*, which encodes bacterio-opsin, apoprotein for the bacteriorhodopsin light-driven proton pump. Thus, in the haloarchaeon NRC-1, as in bacteria, pH adaptation was associated with genes involved in arginine catabolism and proton transport. Our study is among the first to report experimental evolution with multiple resequenced genomes of an archaeon. Haloarchaea are polyextremophiles capable of growth under environmental conditions such as concentrated NaCl and desiccation, but little is known about pH stress. Interesting parallels appear between the molecular basis of pH adaptation in NRC-1 and in bacteria, particularly the acid-responsive arginine-ornithine system found in oral streptococci.

Keywords: *Halobacterium*, Haloarchaea, experimental evolution, acid stress, pH, arginine

INTRODUCTION

Halobacterium sp. NRC-1 (NRC-1) is a polyextremophile that grows optimally at NaCl concentrations in excess of 4 molar (Robinson et al., 2005; DasSarma et al., 2006; Hasan and Mohammadian, 2011; Oren, 2013). A genetically tractable model microbe (Reysenbach and Pace, 1995), it was the first halophilic Archaeon with a fully sequenced genome (Ng et al., 2000). Besides high salt, NRC-1 is capable of surviving: high doses of ionizing radiation and desiccation (Kish et al., 2009), UV radiation (Jones and Baxter, 2017), and toxic ions such as arsenite (Wang et al., 2004). These traits have made NRC-1 a model for studying the possibility of life outside Earth under conditions such as the stratosphere (DasSarma et al., 2017; DasSarma and DasSarma, 2018) or on Mars (DasSarma, 2006; Leuko et al., 2015; DasSarma et al., 2016).

Water on Mars contains high concentrations of salt, as well as acid and iron (Madden et al., 2004). The Mars Exploration Rover Opportunity discovered substantial deposits of an iron hydrous sulfate mineral known as jarosite [$KFe^{3+}_3(OH)_6(SO_4)_2$] which forms in acidic and iron-rich aqueous environments. On earth such conditions occur in acid mine drainage and near volcanic vents. Opportunity's discovery of jarosite on Mars was evidence of acidic, liquid water and an oxidizing atmosphere in the Martian past (Madden et al., 2004; Pritchett et al., 2014). Occurring together, acid and metals can amplify the stress associated with each condition (Dopson et al., 2014). Thus, it is of interest to investigate how a neutrophilic halophile such as NRC-1 (Moran-Reyna and Coker, 2014) might adapt to conditions of acid and high iron.

An informative approach to examine the genomic basis of stress response is experimental laboratory evolution (Lenski et al., 1991; Lenski and Travisano, 1994; Schou et al., 2014; Harden et al., 2015; Tenaillon et al., 2016; Creamer et al., 2017; He et al., 2017). Experimental evolution of bacteria reveals changes in phenotype and genotype in response to specific stressors in a controlled environment, such as carbon source limitation or extreme pH. In bacterial adaptation to various kinds of pH stress, we find a recurring pattern that dominant responses to short-term stress actually decrease fitness over many generations of long-term exposure. For example, amino-acid transport and catabolism play important roles in extreme-acid survival of *Escherichia coli* (Slonczewski et al., 2009; Kanjee and Houry, 2013). However, 2,000 generations of *E. coli* evolution at pH 4.8 select for loss of three acid-inducible amino-acid decarboxylase systems, including arginine decarboxylase (He et al., 2017). As a membrane-permeant acid, benzoic acid induces glutamate decarboxylase and drug resistance regulons, yet these systems are lost or downregulated during experimental evolution (Creamer et al., 2017; Moore et al., 2019). At high external pH, *E. coli* survival requires the stress sigma factor RpoS; however, generations of growth at high pH select against RpoS expression and activity (Hamdallah et al., 2018). It is therefore of interest to investigate whether similar patterns of reversal occur in archaea.

Relatively few experimental evolution studies have been reported in archaea. In NRC-1, serial application of lethal doses

of ionizing radiation selected more resistant mutants that had increased expression of a single-strand DNA binding protein (DeVeaux et al., 2007). In the thermoacidophile *Sulfolobus solfataricus*, serial passage in extreme acid yielded strains that grow below pH 1 (McCarthy et al., 2016). These strains showed mutations in amino acid transporters, as well as upregulation of membrane biosynthesis and oxidative stress response. In *Metallosphaera sedula*, serial passage led to a pH 0.9-adapted strain with four mutations, one of which is an amino-acid/polyamine transporter (Ai et al., 2016). These findings are intriguing, given the role of amino-acid transport and catabolism in extreme-acid survival of bacteria (Slonczewski et al., 2009; Kanjee and Houry, 2013). For example, arginine transport and catabolism, which yields CO₂ plus two ammonium ions, is a prominent response to acid stress of oral streptococci (Dong et al., 2004; Sakanaka et al., 2015).

Archaea employ various processes that involve proton transport via primary pumps and antiporters (Slonczewski et al., 2009; Krulwich et al., 2011; Lund et al., 2014). *Halobacterium* strains possess the light-driven proton pump bacteriorhodopsin (*bop*) that generates proton motive force (PMF) (Simsek et al., 2006; Dummer et al., 2011) as well as several sodium-proton antiporters, which export sodium in exchange for protons (Coker et al., 2007).

The optimal pH range for growth of *Halobacterium* species is pH 7.0–7.5 (Hasan and Mohammadian, 2011). We conducted experimental evolution of NRC-1 under conditions of relatively low pH (pH 6.3–6.5) and at optimal pH for growth (pH 7.5), with high iron versus low iron concentration.

The NRC-1 genome includes a main chromosome and two minichromosomes or megaplasmids (Ng et al., 1998, 2000). It accumulates frequent insertion sequence mutations (ISH) which may mediate rapid adaptations to environmental stress (Sapienza and Doolittle, 1982; DasSarma, 1989). Our study of experimental evolution in a haloarchaeon assesses which mutations contribute to archaeal evolution in acid stress. Here we describe analysis of phenotypic changes across evolved clones from each population, and then use genomic analysis to identify potential underlying mutational bases of these phenotypic responses to selection. Genome analysis of 16 clones revealed a remarkable proportion of events mediated by insertion sequences (ISH). In acid-adapted strains, we found a high frequency of mutations in the arginine-ornithine antiporter *arcD* (Wimmer et al., 2008) and in the associated *arcR* arginine catabolism regulator (Ruepp and Soppa, 1996).

RESULTS

Experimental Evolution Under Conditions of Acid and Iron Stress

Serial culture of evolving populations was conducted as described under Methods (**Supplementary Figure S1**). Populations of NRC-1 were founded from a single clone and cultured in modified CM⁺ medium (Reysenbach and Pace, 1995; Ng et al., 2000) with appropriate buffers to maintain pH. Each population was diluted 500-fold every 4 days (approximately nine

generations). Four independent populations were maintained for each condition: the optimal growth condition, pH 7.5 (designation M); acid stress, initially pH 6.5, later pH 6.3 (designated J); iron amendment, pH 7.5 with 600 μM ferrous sulfate (designated S); and acid with iron amendment (designated K) for a total of 16 experimental populations. Populations evolved under acid stress were cultured at an initial pH of 6.5, which was then lowered to 6.3 at generation 250, as the populations adapted.

After all populations reached 500 doublings, two clones were isolated from each population by three rounds of streaking on CM^+ agar for a total of 32 evolved clones. Genomic DNA was extracted from 16 of these clones, and from the founder stock of NRC-1. DNA samples were sequenced by Illumina MiSeq, and mutations were identified by comparison of the “evolved strain” sequences to that of the NRC-1 ancestral stock, assembled on the reference genome (Ng et al., 2000) using the *breseq* pipeline (Barrick et al., 2014; Deatherage and Barrick, 2014; Deatherage et al., 2015). The strains we characterized are listed in **Table 1**.

Mutations in the Genomes From Evolving Populations

The genomes of the 16 clones were compared to those of the NRC-1 ancestor which we resequenced from our lab stock (**Supplementary Tables S1–S3**). The genome of our NRC-1 stock was also compared to that of the NCBI reference sequence *Halobacterium* sp. NRC-1 (Ng et al., 2000) as shown in **Supplementary Table S4**. A small number of positions differed from that of the reference. Some of these differences are consistent with those of later sequence reports (Pfeiffer et al., 2008, 2019). The sequence differences shown in **Supplementary Table S4** were excluded in our analysis of the evolved clones.

TABLE 1 | Strains used in this study.

Strain Name	Description	Generation	Evolution Condition	Vac +/-*	Source
NRC-1	Ancestor strain	0	–	+	SD
NRC-1	Ancestor strain	0	–	–	SD
JLSHA075	Clone J1	500	pH 6.3	–	This study
JLSHA078	Clone J2-2	500	100 mM PIPES	–	This study
JLSHA079	Clone J3-1	500		+	This study
JLSHA082	Clone J4-2	500		–	This study
JLSHA083	Clone M1	500	pH 7.5	–	This study
JLSHA086	Clone M2-2	500	100 mM MOPS	–	This study
JLSHA087	Clone M3-1	500		+	This study
JLSHA089	Clone M4-1	500		+	This study
JLSHA091	Clone K1	500	pH 6.3	–	This study
JLSHA093	Clone K2-1	500	100 mM PIPES	+	This study
JLSHA095	Clone K3	500	600 μM Fe^{2+}	–	This study
JLSHA097	Clone K4	500		–	This study
JLSHA099	Clone S1	500	pH 7.5	–	This study
JLSHA101	Clone S2	500	100 mM MOPS	–	This study
JLSHA103	Clone S3	500	600 μM Fe^{2+}	–	This study
JLSHA105	Clone S4	500		–	This study

*“+” indicates gas vesicle-forming, “–” indicates non-gas vesicle-forming.

The genomes of the evolved clones had a total of 378 mutations, of which 349 were unique to one strain at the base-pair level. Representative mutations of interest are summarized in **Table 2**. Mutation frequencies were compared for the main replicon and minichromosomes. In total across all resequenced genomes, there were 120 mutations in minichromosome pNRC100, and 171 mutations on minichromosome pNRC200. pNRC100 is about 10% as long as the main chromosome, and pNRC200 is about 20% as long; thus, the two minichromosomes had a mutation frequency more than ten-fold greater than that of the main chromosome, a finding consistent with previous reports of plasmid or minichromosome mutation (Ng et al., 2000).

In the 16 clones, overall, 87 different mutations were found on the main chromosome. Of these, 90% consisted of new ISH positions, or of deletions mobilized by existing ISH elements (**Table 3**). Mutation distributions of the minichromosome replicons showed no significant difference in ISH proportion (94 mutations out of 111, on pNRC100; 141 out of 156 on pNRC200). For comparison, we considered a recent *breseq* analysis of 16 *E. coli* genomes following 500 generations evolution with an organic acid (Moore et al., 2019). Only 18% of the *E. coli* mutations were mediated by insertion sequences. Thus, NRC-1 evolution showed five-fold greater proportion of insertion sequence activity than *E. coli*. Our quantitative analysis of experimentally evolved genomes is consistent with earlier evidence of high ISH activity in halobacterial genomes (DasSarma et al., 1988; DasSarma, 1989; Ng and DasSarma, 1991; Ng et al., 1991, 1993; Pfeiffer et al., 2008).

Haloarchaea including *Halobacterium salinarum* species are known for polyploidy (15–25 genome copies per cell) and for ploidy variation among replicons within a cell (Soppa, 2013). Our evolved clones showed evidence for variable ploidy between and within replicons. Mean read coverage by replicon was modeled by *breseq* (**Table 4**).

Overall, within the ancestor and the evolved clones, the read coverage for the main chromosome was consistent with that of the minichromosome pNRC200. However, the mean coverage of the shorter minichromosome pNRC100 (191 kb) was more than twice that of the main chromosome, for our ancestral NRC-1 and for 12 of the 16 evolved clones. Clones J1, M3-1, K3, S2, and S3 had mean coverage of pNRC100 more than four-fold greater than that of the main chromosome. These high coverage ratios could indicate that our original NRC-1 stock has a double copy number of minichromosome pNRC100, relative to the main chromosome; and that some descendant clones have increased relative copy number. However, the calculations are complicated by wide variation in read coverage between different segments of the same replicon, especially in pNRC100. This variation in read coverage may be caused by internal repeats within the replicon (Ng et al., 1991). Interpretation of the data is complicated by the presence of massive deletions (**Supplementary Table S2**) which comprise up to 50% of the ancestral sequence (for example in clone K1) (Ng et al., 1993). Variation in read coverage could indicate the presence of plasmid copies with different deletion levels within a given polyploid cell.

TABLE 2 | Selected mutations found in evolved clones.*†

Replicon	Start bp	pH 6.3				pH 7.5				pH 6.3, Fe				pH 7.5, Fe				Annotation	Gene Description
		J1	J2-2	J3-1	J4-2	M1	M2-2	M3-1	M4-1	K1	K2-1	K3	K4	S1	S2	S3	S4		
Chromosome	~15,266																	ISH: intergenic	(<i>vng0018H→</i>)/(<i>vng0019H→</i>)
Chromosome	~23,074																	ISH: intergenic	(<i>vng0027H←</i>) / (<i>→vng0028C</i>)
Chromosome	~25,216																	ISH: intergenic	(<i>vng0029H←</i>) / (<i>→vng0030H</i>)
Chromosome	~29,154																	ISH: coding	[<i>vng0032H→</i>]
Chromosome	~48,587																	ISH8-3 mediated	(<i>vng0053H→</i>) / (<i>→vng0053H</i>)
Chromosome	~52,664																	ISH: intergenic	(<i>vng0056H←</i>) / (<i>→vng0057</i> O_{antigen polymerase})
Chromosome	~181,512																	ISH: coding	[<i>vng0215C←</i>]
Chromosome	414,229																	A675A (GCG→GCT)	[<i>vng0053H7←</i>] (TRAP transporter permease)
Chromosome	~749,543																	ISH: coding	[<i>vng0985H→</i>]
Chromosome	~753,552																	ISH: intergenic and (T)9→8	(<i>vng0986H→</i>) / (<i>→vng0987H</i>)
Chromosome	~754,476																	ISH: coding	[<i>vng0939C←</i>] xcd (integrase)
Chromosome	~772,459																	ISH: intergenic	(<i>vng1007H←</i>) / (<i>→vng1003G</i>) flaA1a (flagellin A1 precursor)
Chromosome	~1,089,129																	ISH: coding	[<i>vng1467G→</i>] bop (bacterio-opsin).
Chromosome	~1,229,749																	ISH: coding/ISH2 deletion	[<i>vng1650H←</i>]
PNRC100	0																	ISH7-1 deleted	[<i>vng7001←</i>]-[<i>←vng RS13745</i>]
PNRC100	~9,546																	ISH3-1	[<i>vng RS13755→</i>] / (<i>→vng RS12260</i>)
PNRC100	~14,052																	ISH3-1	(<i>vng_RS12260←</i>) / (<i>→vng7012</i>)
PNRC100	~15,600																	ISH8-3, 8-1	(<i>vng7012→</i>) - (<i>←vng RS12360</i>) Gas vesicle protein cluster (deleted)
PNRC100	~41,820																	ISH5-1*, 8-5	(<i>vng7039→</i>) - (<i>→vng_RS13770</i>) yobE, XRE regulator, MFS transporter, thioredoxin, deoxyribonuclease, cell division control protein (all deleted)
PNRC100	~71,208																	ISH2	(<i>vng_RS13790→</i>) - (<i>←vng7073</i>) SOS response peptidase (deleted)
PNRC100	~75,169																	ISH2	(<i>vng7074←</i>) - (<i>←vng7078</i>)
PNRC100	~81,100																	ISH8-3, 3-1	[<i>vng RS12615←</i>] - (<i>←vng7079</i>)
PNRC100	~83,375																	ISH3-1, 7-2	(<i>vng7080←</i>) - (<i>←vng7085</i>)
PNRC100	~87,224																	V→L(GTG→CTG)	[<i>vng7085←</i>]
PNRC100	~133,744																	ISH8-2, 3-3	(<i>vng_RS12830←</i>) - (<i>→vng7127</i>) Arsenic resistance operon (deleted)
PNRC100	~143,907																	ISH3-3, 2	(<i>vng_RS12880→</i>) - (<i>→vng7136</i>) ssDNA-binding protein A (deleted)
PNRC100	~150,769																	ISH2, 3-2	(<i>vng7136←</i>) / (<i>←vng RS12925</i>)
PNRC100	~152,257																	ISH2, 3-2	[<i>vng RS13345←</i>]

(Continued)

TABLE 2 | Continued

Replicon	Start bp	pH 6.3				pH 7.5				pH 6.3, Fe				pH 7.5, Fe				Annotation	Gene Description
		J1	J2-2	J3-1	J4-2	M1	M2-2	M3-1	M4-1	K1	K2-1	K3	K4	S1	S2	S3	S4		
PNRC100	~153,526																	ISH3-2, 2	[<i>vng_RS13350</i>]
PNRC100	~164,889																	ISH8-5, 5-1	(<i>vng_RS13865</i> ←) – (← <i>vng7170</i>) Thioredoxin reductase, <i>boa3</i> (bacteriorhodopsin activator), <i>phoT1</i> phosphate transporter), <i>cydBA</i> cytochrome doxidase (all deleted).
PNRC200	0																	ISH 7-1 deleted	(<i>vng6001H</i> ←) – [← <i>vng6011H</i>]
PNRC200	~7,477																	ISH: coding	[<i>vng6011H</i> ←]
PNRC200	~9,569																	ISH 3-1	[<i>vng6013G</i> →] / (← <i>vng_RS10565</i>)
PNRC200	~14052																	ISH 3-1	(<i>vng_RS10565</i> ←) / (→ <i>vng6016H</i>)
PNRC200	~15,594																	ISH 8-3, 8-1	(<i>vng6016H</i> →) – (→ <i>vng_RS10665</i>)
PNRC200	~41,819																	ISH 5-1*, 8-5	(<i>vng6053G</i> →) – (→ <i>vng6079H</i>) Thioredoxin reductase, <i>boa3</i> (bacteriorhodopsin activator), <i>phoT1</i> phosphate transporter), <i>cydBA</i> cytochrome doxidase (all deleted).
PNRC200	~71,208																	ISH 2	(<i>vng6094H</i> →) – [← <i>vng6097C</i>] SOS response peptidase (deleted)
PNRC200	~75,168																	ISH 2, 8-4	(<i>vng6099H</i> ←) – (← <i>vng6105H</i>)
PNRC200	~81,101																	ISH 8-4, 3-1	[<i>vng_RS10920</i> ←] / [→ <i>vng_RS10925</i>]
PNRC200	~83,374																	ISH 3-1, 7-2	(<i>vng6112H</i> ←) – [← <i>vng6119H</i>]
PNRC200	~87,224																	V→L(GTG→CTG)	[<i>vng6119H</i> ←]
PNRC200	~138,366																	ISH 8-4	(<i>vng6162H</i> ←) – [→ <i>vng6181H</i>] orc2 (cell division control protein 6), <i>nbp2</i> (nucleic acid binding protein), <i>srl1</i> (ATPase), <i>trkA2</i> (TRK K+ uptake system protein), <i>kdpABC</i> (K+ ATPase), <i>cat3</i> (cationic amino acid transporter) (all deleted).
PNRC200	~140,521																	ISH: coding	[<i>vng6164G</i> ←] orc2 (orc/cell division control protein 6).
PNRC200	~244,149																	ISH: coding	[<i>vng6313G</i> ←] arcD Arginine:ornithine antiporter (formerly annotated <i>nhaC3</i>)
PNRC200	~248,490																	ISH: coding	[<i>vng6318G</i> ←] arcR (Arginine catabolism transcriptional regulator)
PNRC200	~262,599																	ISH 3-2, 8-3 /ISH 8-3 deleted	(<i>vng_RS11B55</i> ←) / (→ <i>vng6331H</i>)
PNRC200	~272,000																	ISH 6, 3-2	(<i>vng6341H</i> →) / (← <i>vng_RS13610</i>)
PNRC200	~274,345																	ISH 3-2, 8-4	(<i>vng_RS11T35</i> ←) / (← <i>vng6345H</i>)

(Continued)

TABLE 2 | Continued

Replicon	Start bp	pH 6.3				pH 7.5				pH 6.3, Fe				pH 7.5, Fe				Gene Description	Annotation
		J1	J2-2	J3-1	J4-2	M1	M2-2	M3-1	M4-1	K1	K2-1	K3	K4	S1	S2	S3	S4		
PNRC200	~278,031																	ISH 8-4, 2	[<i>vng6346H</i> ←] - (← <i>vng6393H</i>) DNA polymerase I, <i>cdc6</i> cell division control protein, HNH endonuclease, MarR family transcriptional regulator, AbrB family transcriptional regulator, L-lactate permease (all deleted)
PNRC200	~278,118																	ISH: coding	[<i>vng6346H</i> ←]
PNRC200	~279,927																	ISH: intergenic	(<i>vng634SH</i> ←) / (← <i>vng6349C</i>)
PNRC200	~293,402																	ISH: coding	[<i>vng6364H</i> ←]
PNRC200	~309,253																	ISH 2, 8-3	(<i>vng6393H</i> ←) - (← <i>vng6395H</i>)
PNRC200	~311,206																	ISH 8-3,11	(<i>vng6396H</i> →) - (← <i>vng6420H</i>) arsR transcriptional regulator, phzF phenazine biosynthesis
PNRC200	~324,384																	ISH 11	(<i>vng_RS12000</i> →) - (→ <i>vng6441H</i>)

* "Annotation" column code: "ISH *** mediated" = flanking ISH elements, if relevant. Mutation codes: blue = missense, green = silent. "Gene" column code: (mutation starts or ends before this gene name), → ← indicates gene directionality, [mutation starts, ends, or is entirely contained within this gene name], "-" indicates intervening omitted genes found in description, "/" indicates mutation is between two genes. Highlight indicates mutations associated with acid evolution. † This chart does not indicate shared lineages through identical mutations. For a complete list of mutations, see **Supplementary Tables S1–S3**.

Acid-Evolved Clone J3-1 Has a Growth Advantage Over a Range of pH Values

After 500 generations of serial culture under four conditions, clones were isolated from the evolving populations. The clones were tested for genetic adaptation under various growth conditions. Each evolved clone was cultured in parallel with the ancestral strain NRC-1. The loss of gas vesicles (*Vac*⁻ phenotype) alters their OD₆₀₀ reading (DasSarma et al., 1988; DasSarma, 1989); for this reason, clones that had lost gas vesicles were cultured in parallel with a *Vac*⁻ isolate of NRC-1 ancestor.

The growth of acid-evolved J-population clones was compared to that of the NRC-1 ancestor (*Vac*⁺) (**Figures 1, 2**). Clone J3-1 reached a significant two-fold higher culture density than did the ancestor when cultured at pH 6.1 or at 6.3 (**Figure 1B**). Growth advantage was seen for all four replicate cultures of J3-1 at pH 6.1 and at pH 6.3, whereas the difference from NRC-1 cultures disappeared at pH 7.2 and at pH 7.5. Thus, strain J3-1 exhibits an acid-specific fitness advantage. The other acid-evolved J-population strains, however, had no significant growth advantage compared to NRC-1, under the conditions tested (**Figure 2**). The acid-adapted strains with high iron (K1-K4) also showed no change in growth rate (**Supplementary Figure S5**).

Acid-Adapted Clones Shared Mutations in *arcD* and in *arcR*

Mutant alleles may confer a fitness advantage at concentrations far below that required to show a difference in growth phenotype (Gullberg et al., 2011, 2014). Therefore, we inspected all acid-adapted strains of NRC-1 for shared mutations, including those without an observable phenotypic change. We inspected the genomes of acid-adapted populations J and K (acid with iron supplement) for mutations in specific genes that were not found in the populations evolved at pH 7.5.

Seven out of eight of the J and K clones (but no M or S clones) had ISH mutations in or upstream of gene VNG_6313G (**Table 2**). This gene was originally classified as encoding a sodium-proton antiporter (*nhaC3*) but was shown instead by physiological experiments to encode an arginine-ornithine antiporter *ArcD* (Ng et al., 1991). PCR amplification and Sanger sequencing of the mutant *arcD* alleles confirmed the presence of insertion sequences ISH2 (strains K1 and K4) and ISH4 (strains J1, K2-1, K3) (**Table 5** and **Supplementary Figure S2**). Additionally, in J4-2, a partial sequence confirms the presence of 1.1 kb ISH11 insertion flanked by a 10 bp direct repeat, while a large 3000 + bp insertion in K3 returned a partial sequence of ISH4. The partial sequence suggests multiple copies of ISH4, or possibly a composite transposon.

Four acid-evolved genomes (J-3, K-1, K2-1, K4-1) and one non-acid-evolved clone (M3-1) possess ISH insertions at different sites in *arcR* on pNRC100 (**Supplementary Table S3**). *ArcR* mediates transcriptional regulation of the *arcABDCR* operon for arginine catabolism (Ruepp and Soppa, 1996; Wimmer et al., 2008). These components include the arginine deiminase (*arcA*), ornithine carbamoyltransferase (*arcB*), carbamate kinase (*arcC*), and the arginine-ornithine antiporter (*arcD*).

TABLE 3 | Classes of mutations found in evolved clones.*

Mutation type	Low pH				Control				Low pH and iron-rich				Iron-rich				Mutation sum
	J1	J2-1	J3-1	J4-2	M1	M2-2	M3-1	M4-1	K1	K2-1	K3	K4	S1	S2	S3	S4	
Chromosome																	
TSD	4	5	3	5	1	4	4	1	7	6	5	5	1	6	6	1	64
Deletion	1	1	0	1	1	1	2	2	1	1	0	1	0	0	1	0	13
SNP	0	0	1	0	1	2	1	1	1	1	0	1	0	0	0	1	10
Insertion	0	0	0	0	0	0	0	0	0	0	0	0	0	0	0	0	0
Chromosome Total	5	6	4	6	3	7	7	4	9	8	5	7	1	6	7	2	87
PNRC100																	
TSD	0	1	0	0	0	7	0	0	3	0	0	0	2	2	0	0	15
Deletion	5	3	4	7	2	0	6	3	17	8	8	10	4	3	5	4	89
SNP	2	0	0	0	0	6	0	0	0	0	3	5	0	0	0	0	16
Insertion	0	0	0	0	0	0	0	0	0	0	0	0	0	0	0	0	0
PNRC 100 Total	7	4	4	7	2	13	6	3	20	8	11	15	6	5	5	4	120
PNRC200																	
TSD	1	1	2	1	1	4	0	0	3	7	3	7	2	0	3	5	40
Deletion	6	4	6	7	8	14	15	7	15	5	4	5	3	5	6	5	115
SNP	1	0	0	0	0	5	0	0	1	0	3	5	0	0	0	0	15
Insertion	1	0	0	0	0	0	0	0	0	0	0	0	0	0	0	0	1
PNRC200 Total	9	5	8	8	9	23	15	7	19	12	10	17	5	5	9	10	171
Complete genome																	
TSD	5	7	5	6	2	15	4	1	13	13	8	12	5	8	9	6	119
Deletion	12	8	10	15	11	15	23	12	33	14	12	16	7	8	12	9	217
SNP	3	0	1	0	1	13	1	1	2	1	6	11	0	0	0	1	41
Insertion	1	0	0	0	0	0	0	0	0	0	0	0	0	0	0	0	1
Complete Total	21	15	16	21	14	43	28	14	48	28	26	39	12	16	21	16	378

*TSD = target site duplication indicating ISH; SNP = single nucleotide polymorphism.

For comparison, a remarkably similar system of arginine catabolism reverses acidification for the periodontal bacterium *Streptococcus gordonii* (Dong et al., 2004; Sakanaka et al., 2015).

TABLE 4 | Coverage depth for NRC-1 and evolved clones.

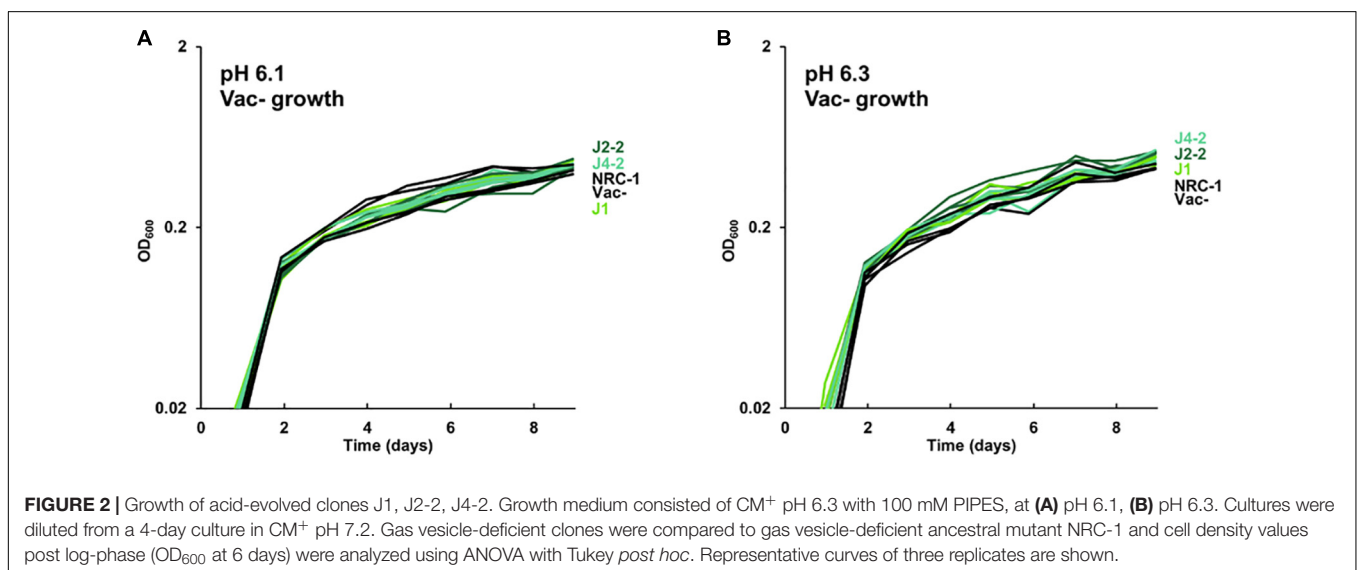
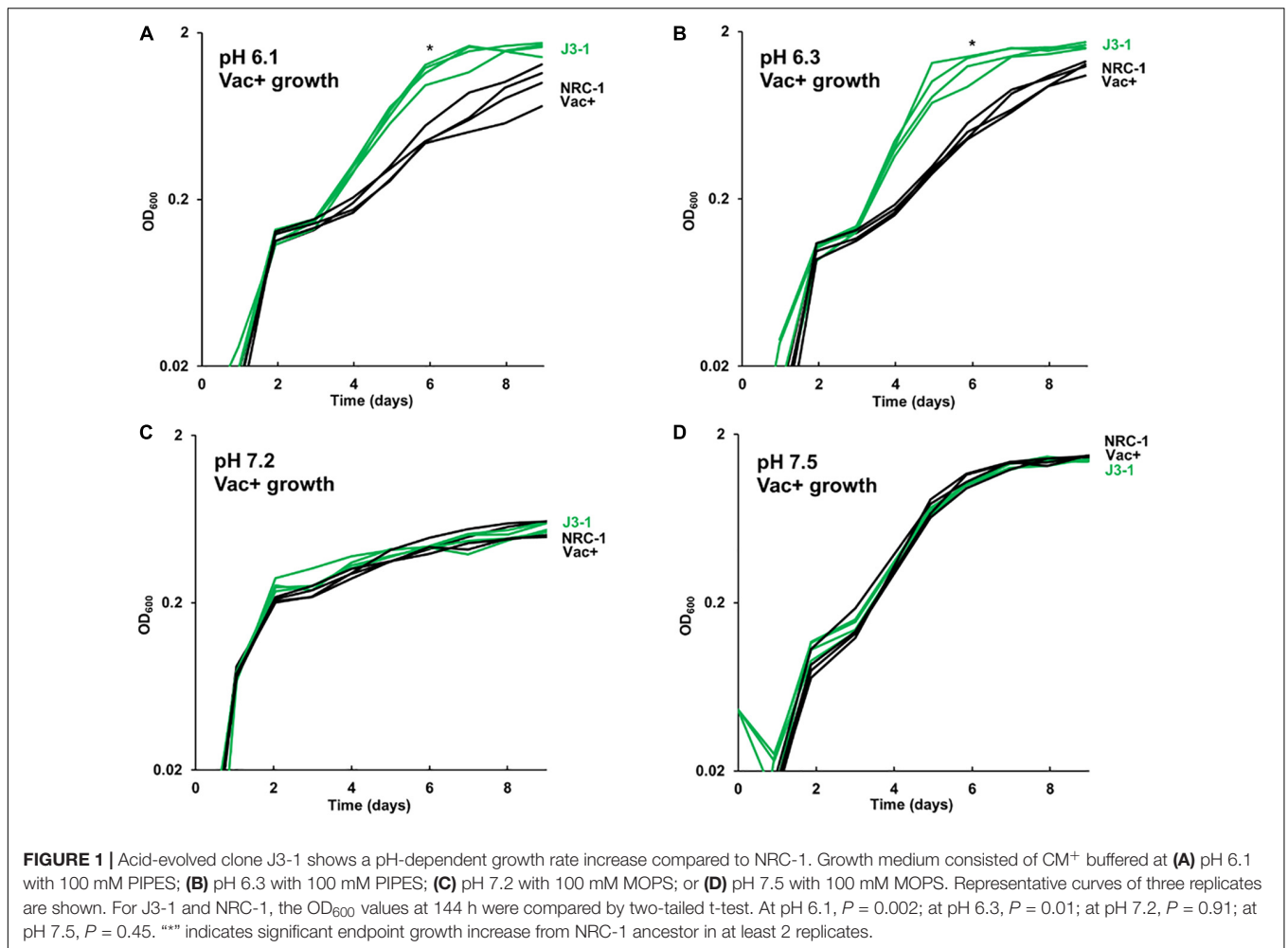
Strain	Main chromosome		pNRC100		pNRC200	
	Read depth*	SD	Read depth*	SD	Read depth*	SD
NRC-1	50	10	128	15	64	10
J1	46	9	338	29	53	9
J2-2	41	9	156	14	48	8
J3-1	57	11	87	13	91	14
J4-2	64	11	137	15	85	13
M1	49	9	187	18	44	7
M2-2	67	11	165	17	62	10
M3-1	49	10	275	26	54	9
M4-1	65	11	162	13	75	11
K1	74	13	72	10	63	11
K2-1	72	13	NA	NA	76	11
K3	52	10	363	29	92	13
K4	59	11	96	11	71	15
S1	39	8	125	15	44	8
S2	42	9	169	18	34	7
S3	47	10	202	16	55	9
S4	46	9	185	14	37	7

*Mean copy number of sequence across the replicon, according to the *bresseq* fitted dispersion model. SD = standard deviation predicted by the model.

Arginine catabolism releases CO₂ and two molecules of ammonia, which cause net alkalization. The system mediates tooth biofilm formation by *S. gordonii*. For *E. coli*, the arginine decarboxylase *Adi* reverses acidification at extreme low pH (Gong et al., 2003). The *adi* system of *E. coli* is induced by acid stress but largely lost by insertion-sequence mutations after long-term evolution in acid (Harden et al., 2015; Creamer et al., 2017). This suggests a model for acid adaptation in haloarchaea that is remarkably similar to that observed in *E. coli*, in which acid-stress adaptations are knocked down by long-term acid exposure (He et al., 2017).

Acid-Adapted Clones Shared Mutations in Bacteriorhodopsin (*bop*)

In NRC-1, our acid-evolved clones J3-1 and K1 each contained an ISH element in the gene *bop* that encodes the light-driven proton pump bacteriorhodopsin (Simsek et al., 2006). The J3-1 allele was confirmed by Sanger sequence as a 1.1 kb insertion of ISH1 with an eight bp target site duplication in *bop* (Table 5 and Supplementary Table S1). This exact mutation has been previously studied in bacteriorhodopsin mutants, and was in fact the first transposable element identified in haloarchaea (Simsek et al., 2006). This particular target site duplication was shared with acid-evolved clone K1. At a different position, a *bop* ISH insertion was found in one of the M population clones (M3-1) which had not undergone acid selection, consistent with previous spontaneous insertions in this gene.



The *bop* and *arcD* mutations were found together in J3-1, but also in acid-adapted K1, which did not show a significant phenotype under our conditions tested. We inspected strain J3-1

for candidate mutations that might be responsible for this strain's unique degree of adaptation at low pH. Overall, the J3-1 genome had 16 mutations compared to the NRC-1 ancestor (Table 6).

TABLE 5 | ISH insertions confirmed by PCR in acid-adapted strains.

Strain	Gene mutation	ISH	Primer 1	Primer 2
J1	<i>arcD</i> insertion	ISH4	GATAACGATGGACATGTACT	GTCGGTATCGTTCCTTTGGG
J3-1	<i>arcR</i> insertion	ISH8-2	ACTGGTGTGGAGTTTCCGTG	ATCTCACGATCAAGGACGGTGT
J3-1	<i>bop</i> insertion	ISH1	GAGTTACACACATATCCTCG	GCGTAGAATTTCTTGCATC
J4-2	<i>arcD</i> insertion	ISH11	GATAACGATGGACATGTACT	GTCGGTATCGTTCCTTTGGG
K1	<i>arcD</i> insertion	ISH2	GATAACGATGGACATGTACT	GTCGGTATCGTTCCTTTGGG
K1	<i>arcR</i>	ISH8-2	ACTGGTGTGGAGTTTCCGTG	ATCTCACGATCAAGGACGGTGT
K2-1	<i>arcD</i> insertion	ISH4	GATAACGATGGACATGTACT	GTCGGTATCGTTCCTTTGGG
K3	<i>arcD</i> insertion	ISH4	GATAACGATGGACATGTACT	GTCGGTATCGTTCCTTTGGG
K4	<i>arcD</i> insertion	ISH2	GATAACGATGGACATGTACT	GTCGGTATCGTTCCTTTGGG
K4	<i>arcR</i>	ISH3-2	AGAAGTCGTTCCAGAAACAGG	GATACGCGATCAACGACGA

TABLE 6 | Acid-evolved clone J3-1 mutations.*[‡]

Replicon	Start bp	End bp	Mutation	Annotation	Gene description
Chromosome	749,943	749,954	(11 bp)1→2	ISH: coding (562/2007 nt)	[<i>vng0985H</i> →]
Chromosome	1,089,129	1,089,137	(8 bp)1→2	ISH: coding (15/789 nt)	[<i>vng1467G</i> →] bop (bacterio-opsin).
Chromosome	1,163,363		A→G	K197R (AA→AG)	[<i>vng1561</i> →] Ferredoxin
Chromosome	1,229,749	1,229,760	(11 bp)1→2	ISH: coding (582/849 nt)	In <i>vng1650</i>
PNRC100	0	7,788	Δ7788 bp	ISH7-1 deleted	[<i>vng7001</i> ←] – [← <i>vng_RS13745</i>]
PNRC100	71,210	74,656	Δ3447 bp	ISH2 mediated	(<i>vng_RS13790</i> →) – [← <i>vng7073</i>] SOS response peptidase (deleted)
PNRC100	133,743	142,521	Δ8779 bp	ISH8-2, 3-3 mediated	(<i>vng_RS12330</i> ←) – (→ <i>vng7127</i>) Arsenic resistance operon (deleted)
PNRC100	143,909	150,253	Δ6345 bp	ISH3-3, 2 mediated	(<i>vng_RS12880</i> →) – [→ <i>vng7136</i>] ssDNA-binding protein A (deleted)
PNRC200	0	7,760	Δ7760 bp	ISH 7-1 deleted	(<i>vng6001H</i> ←) – [← <i>vng6011H</i>]
PNRC200	71,219	74,595	Δ3377 bp	ISH 2 mediated	(<i>vng6094H</i> →) – [← <i>vng6097C</i>] SOS response peptidase (deleted)
PNRC200	244,422	244,430	9 bp(1→2)	ISH: intergenic	[<i>vng6313G</i> ←] / (<i>vng6315G</i> ←) arcD Arginine:ornithine antiporter/ornithine carbamoyltransferase
PNRC200	249,147	249,157	11 bp(1→2)	ISH: coding	[<i>vng6318G</i> ←] arcR Arginine catabolism transcription a I regulator
PNRC200	262,603	265,437	Δ2835 bp	ISH 3-2, 8-3 mediated/ ISH 8-3 deleted	(<i>vng_RS11685</i> ←) / (→ <i>vng6331H</i>)
PNRC200	309,256	309,812	Δ557 bp	ISH 2, 8-3 mediated	(<i>vng6393H</i> ←) – (← <i>vng6395H</i>)
PNRC200	311,213	323,320	Δ12108bp	ISH 8-3, 11 mediated	(<i>vng6396H</i> →) – (← <i>vng6420H</i>) arsR transcriptional regulator, phzF phenazine biosynthesis
PNRC200	324,386	332,792	Δ8407 bp	ISH 11 mediated	(<i>vng_RS12000</i> →) – (→ <i>vng6441H</i>)

* "Annotation" column code: "ISH *** mediated" = flanking ISH elements, *missense mutations in blue*. "Gene" column code: (mutation starts or ends before this gene name), → ← indicates gene directionality, [mutation starts, ends, or is entirely contained within this gene name], "-" indicates intervening omitted genes found in description, "/" indicates mutation is between two genes. [‡]Highlight indicates mutations associated with acid evolution.

Of these, only one mutation affected a gene not affected in any other evolved clone. This is a missense mutation in a ferredoxin gene (*VNG1561*) resulting in a conservative change from lysine to arginine. Mutations were also found affecting several proteins involved in transcriptional regulation, which in combination might contribute to the acid fitness phenotype.

Clones Evolved at pH 7.5 Show No Increase in Relative Fitness

All evolved clones from generation 500 with *Vac*⁻ phenotypes were grown over 200 h in unbuffered *CM*⁺ medium without acid or iron amendment and compared to the growth phenotype of

the NRC-1 *Vac*⁻ control strain (**Supplementary Figure S2A**). Similarly, the growth phenotypes in unstressed medium of *Vac*⁺ clones from the 500-generation populations that retained them were compared to that of the NRC-1 *Vac*⁺ ancestor (**Supplementary Figure S2B**). None of the M populations show a significant growth advantage compared to the ancestral strain (**Supplementary Figures S3A,B**).

Growth curves were also conducted for clones from the S populations (evolved with 600 μM *FeSO*₄). Media contained *CM*⁺ pH 7.5 with 100 mM MOPS and 600 μM *FeSO*₄. All evolved clones were persistent *Vac*⁻ mutants at generation 500 and were therefore compared to an NRC-1

Vac⁻ control (**Supplementary Figure S4**). No significant differences were observed.

Multiple Clones Lost Gas Vesicles and Arsenic Resistance

Under laboratory conditions, gas vesicle-producing (Vac⁺) NRC-1 clones have high rates of spontaneous mutation to a vesicle-deficient (Vac⁻) phenotype due to mutations in *gvp* on pNRC100 (DasSarma et al., 1988; DasSarma, 1989). Twelve out of sixteen of our evolved clones, including representatives of each selection type, had lost genes required for gas vesicle nanoparticle production (*gvp*) (DasSarma et al., 1994, 2012; DasSarma and Arora, 1997). Cultures were oxygenated continually by rotating in a bath, effectively eliminating the competitive advantage of producing gas vesicles in oxygen-limiting environments. Thus, as expected, many insertions and deletions were found that had eliminated gas vesicles (DasSarma et al., 1988; Pfeiffer et al., 2008). We characterized gas vesicle phenotypes every 100 generations for the stressed condition populations. These Vac phenotypes (loss of gas vesicle nanoparticles) are presented by population and organized by respective evolution condition in **Table 7**. All evolving populations showed loss of gas vesicle production in some cells. By generation 500, the Vac⁻ phenotype was prevalent in all populations. There was no significant correlation with pH or with iron amendment.

In addition, 13/16 evolved clones had lost the major arsenic resistance operon (*ars*) encoded on pNRC100 (Wang et al., 2004). Other mutations affecting transcriptional regulators and initiation factors occurred in parallel across multiple populations. These and other parallel mutations are summarized in **Table 2**. Various hot spots for mutation appear, many of which are caused by ISH insertions or ISH-mediated deletions.

DISCUSSION

Here, we report one of the first evolution experiments to be conducted on a haloarchaeon. A previous evolution experiment involves selection of mutants resistant to ionizing radiation (DeVeaux et al., 2007).

We compared four environmental conditions: low pH versus optimal pH 7.5, with or without iron supplementation. Overall, in the 500-generation evolved strains, we found a striking pattern of large ISH-mediated deletions, particularly in the two minichromosomes (**Supplementary Tables S1–S3**). For comparison, in *E. coli*, experimental evolution for 2,000 generations at low pH yields only occasional large deletions (Creamer et al., 2017; He et al., 2017). However, after just 500 generations of evolution in the haloarchaeon NRC-1, every evolved clone contained several large-scale deletions. ISH insertion mutations greatly outnumbered SNPs. These types of changes reflect frequent DNA rearrangements and genetic variability observed previously in NRC-1 (Sapienza and Doolittle, 1982; Ng et al., 1991; Simsek et al., 2006).

The acid-adapted NRC-1 populations showed a striking prevalence of mutations affecting the *arcD* and *arcR* components of arginine transport and catabolism. Arginine catabolism with

TABLE 7 | Change in gas vesicle phenotype during evolution across populations.*

Media condition	Populations	Generation				
		100	200	300	400	500
pH 6.3 100 mM PIPES	J1	+	Vac ^{+/-}	–	–	–
	J2	+	Vac ^{+/-}	–	–	Vac ^{+/-}
	J3	> 1% Vac ⁻	Vac ^{+/-}	–	–	Vac ^{+/-}
	J4	+	+	–	–	Vac ^{+/-}
pH 7.5 100 mM MOPS	M1	+	+	+	Vac ^{+/-}	Vac ^{+/-}
	M2	+	+	+	Vac ^{+/-}	Vac ^{+/-}
	M3	+	+	+	Vac ^{+/-}	Vac ^{+/-}
	M4	+	> 1%Vac ⁻	+	+	Vac ^{+/-}
pH 6.3 100 mM PIPES 600 μM FeSO ₄	K1	+	Vac ^{+/-}	–	Vac ^{+/-}	Vac ^{+/-}
	K2	Vac ^{+/-}	Vac ^{+/-}	–	–	Vac ^{+/-}
	K3	+	Vac ^{+/-}	–	–	Vac ^{+/-}
	K4	+	Vac ^{+/-}	–	–	Vac ^{+/-}
pH 7.5 100 mM MOPS 600 μM FeSO ₄	S1	+	+	–	–	–
	S2	+	+	–	–	–
	S3	+	+	–	–	–
	S4	+	+	–	–	–

*“+” indicates gas vesicle-forming, “–” indicates non-gas vesicle-forming.

ammonia release plays a major role in reversing acidity for Gram-positive and Gram-negative bacteria. It is striking to see how the role of acid-dependent arginine catabolism may extend to haloarchaea. The arginase/arginine deiminase family (COG0010) represents a set of orthologs proposed to be among those transferred horizontally to archaea from an ancient bacterial ancestor (Nelson-Sathi et al., 2012).

The ISH insertions seen in acid-adapted clones would be expected to knock out the arginine system, as seen in *E. coli* experimental evolution with acid (Ruepp and Soppa, 1996; Creamer et al., 2017). The reason for the evolutionary loss is proposed to be a readjustment to long-term acid exposure, for which the sustained induction of arginine catabolism becomes counterproductive. It is interesting to find evidence for a similar evolutionary mechanism in a haloarchaeon.

In addition, the acid-evolved strains J3-1 and K1 show an identical insertion mutation affecting the bacteriorhodopsin *bop* gene. The loss of *bop* may be neutral or advantageous under low external pH, where a high PMF already exists. The bacteriorhodopsin pump could be a source of proton leakage at high PMF.

The acid-fitness advantage of clone J3-1 could arise from a single mutation unique to J3-1, such as the missense mutation in a ferredoxin that is unique to J3-1. More likely, however, acid fitness arises from a cumulative effect of loss of function mutations in a number of other genes including *arcA*, *arcR*, and *bop*. It is possible that some unknown factor accounts for the acid-fitness phenotype exhibited by J3-1 under the conditions tested. Nonetheless, it is interesting that the three genes with mutations prevalent in acid-evolved strains all encode products involved in proton consumption or export.

Our findings support previous reports of the importance of ISH elements in haloarchaeal evolution (Pfeiffer et al., 2008), and the observations in *Sulfolobus* that large deletions and loss of function mutations are fitness tradeoffs for surviving in stressful environments (Redder and Garrett, 2006). Large deletions and IS insertions are also common in experimental evolution of bacteria (Creamer et al., 2017; He et al., 2017; Griffith et al., 2018; Hamdallah et al., 2018). We also find evidence for accumulation of ploidy changes for the shorter minichromosome, pNRC100 (Soppa, 2013). We show that experimental evolution is an effective approach to identify candidate genes for environmental stress response in a haloarchaeon.

MATERIALS AND METHODS

Halobacterium Strains and Media

All evolved clones were derived from a stock of *Halobacterium* sp. NRC-1 from the laboratory of Shiladitya DasSarma (Ng et al., 2000). Liquid cultures were grown in Complex Medium Plus Trace Metals (CM⁺) based on Ref (Reysenbach and Pace, 1995), Protocol 25: 250 g/l NaCl, 20 g/l MgSO₄·7H₂O, 2 g/l KCl, 3 g/l Na₃C₆H₅O₇·2H₂O, 10 g/l Oxoid Peptone, and 100 μl/l Trace Metals (3.5 g/l FeSO₄·7H₂O, 0.88 g/l ZnSO₄·7H₂O, 0.66 g/l MnSO₄·H₂O, and 0.2 g/l CuSO₄·5H₂O dissolved 0.1M HCl) with supplements as needed for the conditions examined (Berquist et al., 2006). CM⁺ solid medium included addition of 20 g/l granulated agar. All cultures were incubated at 42°C with rotation. This temperature lies within the organism's optimal growth range of 31–49°C (Robinson et al., 2005). Cultures on solid media were incubated at 42°C for 7–10 days until colonies reached approximately 1 mm in diameter. A Vac⁻ mutant of our NRC-1 stock culture was obtained by picking a Vac⁻ colony followed by three restreaks on CM⁺ agar.

Liquid CM⁺ media for experimental evolution was made with either 100mM PIPES (pKa = 6.8) or 100mM MOPS (pKa = 7.2) buffer with pH adjusted using 5 M NaOH or 5 M HCl as needed, followed by filter sterilization. 100 mM FeSO₄ stock was prepared in deionized water and filter-sterilized before every other dilution during serial batch culture evolution. Sterilized FeSO₄ stock was added to buffered CM⁺ after filter sterilization. For freezer stocks, live cultures were mixed 1:1 with a 50% glycerol, 50% complex medium basal salts mixture as a cryoprotectant. Complex medium basal salts were 250 g/l NaCl, 20 g/l MgSO₄·7H₂O, 2 g/l KCl, 3 g/l Na₃C₆H₅O₇·2H₂O. Acidic, control, iron-rich and acidic, and iron-rich media used in the evolution consisted of: CM⁺ pH 6.5 with 100 mM PIPES (populations J1-J4), CM⁺ pH 7.5 with 100 mM MOPS (populations M1-M4), CM⁺ pH 6.5 (or pH 6.3) with 100 mM PIPES 600 μM FeSO₄ (populations K1-K4), and CM⁺ pH 7.5 with 100 mM MOPS 600 μM FeSO₄ (populations S1-S4).

Experimental Evolution

A total of 16 populations (four per evolution condition) were founded from a 5 ml CM⁺ tube culture (4–5 days incubation) of *Halobacterium* sp. NRC-1 that was diluted 500-fold and incubated 4 days in a 42°C shaker bath at 200 rpm. At the end

of the fourth day, 10 μl of the previous culture was diluted into 5 ml of fresh CM⁺ media amended as necessary for the respective stress condition. The resulting 1:500 dilutions yield approximately nine generations per dilution cycle. If cultures did not reach a healthy cell density as qualitatively evaluated for each dilution, 1:100 or 1:250 dilutions were performed to prevent loss of evolving populations. Alternative dilution concentrations were factored into total generation counts at the end of experimental evolution. When evolution was interrupted, the populations were revived by 1:250 dilutions from freezer stocks of the previous dilution. Freezer stocks comprised 1 ml liquid, mature haloarchaea culture for each evolving population and 0.5 ml glycerol/basal salts mixture, stored in 2 ml Wheaton brand vials and frozen at –80°C for each dilution, totaling 16 freezer stocks every 4 days. A summary of the evolution procedure is presented in **Supplementary Figure S1**.

Clone Selection

Clones were isolated by plating 10 μl of culture from generation 100, 200, 300, 400, and 500 from freezer stocks for all 16 evolving populations on CM⁺ agar plates, followed by incubation in a sealed container at 42°C for 7–10 days. Isolated colonies were then selected for diverse Vac phenotypes, streaked on fresh CM⁺ agar plates, and incubated a second time. The process was repeated a third time to ensure isolation of select genetically pure clones. Colonies from the third streak were grown in unbuffered CM⁺ pH 7.2, and stocks were frozen for later phenotype and genotype characterization. One clone was isolated from each population every 100 generations. For populations that presented mixed gas vesicle production phenotypes, we isolated both a Vac⁺ clone and a Vac⁻ clone. In total, 75 clones were isolated from generation 100, 200, 300, and 400 of the evolution. Clones were similarly isolated from generation 500; however, the first streak was taken directly from evolving populations, rather than from frozen stock in Wheaton vials. Two clones were isolated from each population at 500 generations, for a total of 32 clones.

Gas Vesicle Formation Phenotype Analysis

Vesicle formation phenotype was assessed qualitatively based on the relative translucence of plated colonies and denoted as Vac⁺ or Vac⁻ as appropriate (DasSarma et al., 1988; Reysenbach and Pace, 1995). If more than one Vac phenotype was observed in a streak during strain isolation, the phenotypic variant colonies were re-streaked and treated as separate clonal isolates. Vac phenotypes were evaluated for persistence with each streak based on whether or not Vac⁺ colonies yielded > 1% Vac⁻ progeny or vice versa.

Growth Assays

The generation 500 clones used in these assays are summarized in **Table 1**. Clones were cultured in unbuffered CM⁺ at pH 7.2, and incubated for 4 days in a 42°C shaker bath with 200 rpm orbital aeration. Over-week starter cultures were diluted 1:1000 into new test tubes with 5 ml of the appropriate test condition media. A media blank was included for each

media condition, and each clone was tested with four to eight biological replicates, depending on the assay. Immediately after inoculation, OD₆₀₀ values were recorded by a Spectramax Plus 384 spectrophotometer at 600 nm using Softmax Pro version 6.4.2. Daily readings were taken for 9 days. Media for these tests included CM⁺ pH 6.3 100 mM PIPES and CM⁺ pH 6.1 100 mM PIPES for J clones. M clones were tested in CM⁺ pH 7.5 100 mM MOPS. K clones were tested in CM⁺ pH 6.3 100 mM PIPES 600 μM FeSO₄ and CM⁺ pH 6.1 100 mM PIPES 600 μM FeSO₄. S clones were tested in CM⁺ pH 7.5 100 mM MOPS 600 μM FeSO₄.

To test for pH-dependent growth advantages, evolved clones that showed growth advantages over ancestor in their respective evolution stress conditions under which they were evolved were also tested for growth advantages in pH conditions other than those in which they evolved. For these experiments, J3-1 was cultured in CM⁺ pH 7.5 100 mM MOPS and compared using a Vac⁺ NRC-1 control, M3-1 was cultured in CM⁺ pH 6.1 100 mM PIPES and compared using a Vac⁺ NRC-1 control, and K2-1 was cultured in CM⁺ pH 7.5 100 mM MOPS 600 μM FeSO₄ and compared to both Vac⁺ and Vac⁻ NRC-1 controls due to gas vesicle phenotype ambiguity. Analysis was carried out with comparisons to an ancestral control expressing the same Vac phenotype as the evolved clone.

All growth assays were evaluated for statistical significance using ANOVA test with Tukey *post hoc* or paired T-test using base R and agricolae package. Comparisons between clones were made using post log-phase endpoint “E” values for optical density at 6 days post inoculation.

DNA Extraction and Genome Sequencing

Genomic DNA was isolated from the 16 evolved clones and the ancestor NRC-1 using an Epicentre MasterPure Gram Positive DNA Extraction Kit and a modified procedure. Lysozyme was omitted, and DNA purity and concentration was determined using a Thermo Scientific NanoDrop 2000. Genomic DNA was sequenced at the Michigan State University Research Technology Support Facility (RTSF) Genomics Core. Libraries were prepared using the Illumina TruSeq Nano DNA library preparation kit for Illumina MiSeq sequencing and loaded on a MiSeq flow cell after library validation and quantitation. Sequencing was completed using a 2- by 250-bp paired-end format using Illumina 500 cycle V2 reagent cartridge. Illumina Real Time Analysis (RTA) v1.18.54 performed base calling, and the output of the RTA was demultiplexed and converted to FastQ format with Illumina Bcl2fastq v1.8.4.

Sequence Assembly and Analysis Using the *breseq* Computational Pipeline

The computational pipeline *breseq* version 0.27.1 was used to assemble and annotate the resulting Illumina reads of the evolved clones (Barrick et al., 2014; Deatherage and Barrick, 2014; Deatherage et al., 2015). The current *breseq* version is optimized to detect IS element insertions and IS-mediated deletions, as well as SNPs and other mutations in *E. coli* (Tenailon et al., 2016). Illumina reads were mapped to the *Halobacterium* sp.

NRC-1 reference genome (NCBI GenBank assembly accession GCA_000006805.1). Mutations were predicted by *breseq* through sequence comparisons between the evolved and ancestral clones.

The Integrative Genomics Viewer (IGV) from the Broad Institute at Massachusetts Institute of Technology was used to visualize the assembly and mutations in the evolved clonal sequences mapped to the reference NRC-1 genome (Thorvaldsdóttir et al., 2013). Each replicon was mapped separately using the following RefSeq IDs: NC_002607.1 (main chromosome), NC_001869.1 (pNRC100), and NC_002608.1 (pNRC200). Sequence mean coverage in each evolved clone was estimated using the *breseq* fit dispersion function.

PCR Confirmation of ISH Insertions

PCR primers (Table 5) were designed to confirm the presence of insertion sequences at hypothetical target site duplications. Primers adhered to the following specifications using Sigma Aldrich Oligo Evaluator: 19–22 bp in length, GC content between 40 and 60%, no single bp runs > 3, weak to no secondary structure, and no primer dimer. Oligos were checked for sequence identity of ≤13 bp to any part of the NRC-1 genome other than the target site using NCBI BLAST. We ran 50-μl PCR using Applied Biosystems Amplitaq Gold 360 Master Mix according to the package insert with GC enhancer. To assess insert length, 10 μl of PCR product was electrophoresed in a 1% agarose gel. PCR products were then purified either by Qiagen QIAquick PCR Purification Kit or QIAquick Gel Extraction Kit.

DATA AVAILABILITY STATEMENT

Sequenced genomes are deposited at NCBI under SRA accession number SRP195828. <https://www.ncbi.nlm.nih.gov/sra/SRP195828>.

AUTHOR CONTRIBUTIONS

KK designed the study, performed most of the experiments, and drafted the manuscript. JG co-designed the study and performed many of the experiments. CH conducted growth curves and analyzed resequenced genomes. KB conducted growth curves and analyzed genomes. HL conducted growth curves. PD advised and trained students on haloarchaea procedures. SD mentored and trained students, and contributed to study design. JS conceived the central concept, mentored students, and completed the manuscript.

FUNDING

This project was supported by the National Science Foundation award MCB-1613278 to JS, the 2016 NASA Astrobiology Program Early Career Collaboration Award to KK and JG, and NASA Exobiology grant 80NSSC19K0463 to SD.

ACKNOWLEDGMENTS

We thank Friedhelm Pfeiffer for pointing out the *arcD* annotation. We thank Landon Porter, Wolf Pecher, and Victoria Laye for expert technical assistance.

REFERENCES

- Ai, C., McCarthy, S., Eckrich, V., Rudrappa, D., Qiu, G., and Blum, P. (2016). Increased acid resistance of the archaeon, *Metallosphaera sedula* by adaptive laboratory evolution. *J. Ind. Microbiol. Biotechnol.* 43, 1455–1465. doi: 10.1007/s10295-016-1812-0
- Barrick, J. E., Colburn, G., Deatherage, D. E., Traverse, C. C., Strand, M. D., Borges, J. J., et al. (2014). Identifying structural variation in haploid microbial genomes from short-read resequencing data using breseq. *BMC Genomics.* 15:1039. doi: 10.1186/1471-2164-15-1039
- Berquist, B. R., Müller, J. A., and DasSarma, S. (2006). 27 genetic systems for halophilic archaea. *Methods Microbiol.* 35, 649–680. doi: 10.1007/s00792-015-0794-6
- Coker, J. A., DasSarma, P., Kumar, J., Müller, J. A., and DasSarma, S. (2007). Transcriptional profiling of the model archaeon *Halobacterium* sp. NRC-1: responses to changes in salinity and temperature. *Saline Systems* 3:6. doi: 10.1186/1746-1448-3-6
- Creamer, K. E., Ditmars, F. S., Basting, P. J., Kunka, K. S., Hamdallah, I. N., Bush, S. P., et al. (2017). Benzoate- and salicylate-tolerant strains of *Escherichia coli* K-12 lose antibiotic resistance during laboratory evolution. *Appl. Environ. Microbiol.* 83:e02736. doi: 10.1128/AEM.02736-16
- DasSarma, P., and DasSarma, S. (2018). Survival of microbes in Earth's stratosphere. *Curr. Opin. Microbiol.* 43, 24–30. doi: 10.1016/j.mib.2017.11.002
- DasSarma, P., Laye, V. J., Harvey, J., Reid, C., Shultz, J., Yarborough, A., et al. (2017). Survival of halophilic archaea in Earth's cold stratosphere. *Int J Astrobiol.* 16, 321–327. doi: 10.1017/s1473550416000410
- DasSarma, P., Tuel, K., Nierenberg, S. D., Phillips, T., Pecher, W. T., Nrc-, H., et al. (2016). Inquiry-driven teaching & learning using the archaeal microorganism *Halobacterium*. *Am. Biol. Teach.* 78, 7–13.
- DasSarma, P., Zamora, R. C., Müller, J. A., and DasSarma, S. (2012). Genome-wide responses of the model archaeon *Halobacterium* sp. strain NRC-1 to oxygen limitation. *J. Bacteriol.* 194, 5530–5537. doi: 10.1128/jb.01153-12
- DasSarma, S. (1989). Mechanisms of genetic variability in *Halobacterium halobium*: the purple membrane and gas vesicle mutations. *Can. J. Microbiol.* 35, 65–72. doi: 10.1139/m89-010
- DasSarma, S. (2006). Extreme halophiles are models for astrobiology. *Microbe* 1, 120–126. doi: 10.1128/microbe.1.120.1
- DasSarma, S., and Arora, P. (1997). Genetic analysis of the gas vesicle gene cluster in haloarchaea. *FEMS Microbiol. Lett.* 153, 1–10. doi: 10.1186/1472-6750-13-112
- DasSarma, S., Arora, P., Lin, F., Molinari, E., and Yin, L. R. S. (1994). Wild-type gas vesicle formation requires at least ten genes in the *gvp* gene cluster of *Halobacterium halobium* plasmid pNRC100. *J. Bacteriol.* 176, 7646–7652. doi: 10.1128/jb.176.24.7646-7652.1994
- DasSarma, S., Berquist, B., Coker, J., DasSarma, P., and Müller, J. (2006). Post-genomics of the model haloarchaeon *Halobacterium* sp. NRC-1. *Saline Systems.* 2:3.
- DasSarma, S., Halladay, J. T., Jones, J. G., Donovan, J. W., Giannasca, P. J., and de Marsac, N. T. (1988). High-frequency mutations in a plasmid-encoded gas vesicle gene in *Halobacterium halobium*. *Proc. Natl. Acad. Sci. U.S.A.* 85, 6861–6865.
- Deatherage, D. E., and Barrick, J. E. (2014). Identification of mutations in laboratory-evolved microbes from next-generation sequencing data using breseq. *Methods Mol. Biol.* 1151, 165–188. doi: 10.1007/978-1-4939-0554-6
- Deatherage, D. E., Traverse, C. C., Wolf, L. N., and Barrick, J. E. (2015). Detecting rare structural variation in evolving microbial populations from new sequence junctions using breseq. *Front. Genet.* 5:468. doi: 10.3389/fgene.2014.00468
- DeVaux, L. C., Müller, J. A., Smith, J., Petrisko, J., Wells, D. P., and DasSarma, S. (2007). Extremely radiation-resistant mutants of a halophilic archaeon with increased single-stranded DNA-binding protein (RPA) gene expression. *Radiat Res.* 168, 507–514.
- Dong, Y., Chen, Y. Y. M., and Burne, R. A. (2004). Control of expression of the arginine deiminase operon of *Streptococcus gordonii* by CcpA and Flp. *J. Bacteriol.* 186, 2511–2514. doi: 10.1128/jb.186.8.2511-2514.2004
- Dopson, M., Ossandon, F. J., Lövgren, L., and Holmes, D. S. (2014). Metal resistance or tolerance? Acidophiles confront high metal loads via both abiotic and biotic mechanisms. *Front. Microbiol.* 5:157. doi: 10.3389/fmicb.2014.00157
- Dummer, A. M., Bonsall, J. C., Cihla, J. B., Lawry, S. M., Johnson, G. C., and Peck, R. F. (2011). Bacteriopsin-mediated regulation of bacterioruberin biosynthesis in *Halobacterium salinarum*. *J. Bacteriol.* 193, 5658–5667. doi: 10.1128/JB.05376-11
- Gong, S., Richard, H., and Foster, J. W. (2003). YjdB (AdiC) is the arginine:agmatine antiporter essential for arginine-dependent acid resistance in *Escherichia coli*. *J. Bacteriol.* 185, 4402–4409. doi: 10.1128/jb.185.15.4402-4409.2003
- Griffith, J. M., Basting, P. J., Bischof, K. M., Wrona, E. P., Kunka, K. S., Tancredi, A. C., et al. (2018). Experimental evolution of *Escherichia coli* K-12 in the presence of proton motive force (PMF) uncoupler carbonyl cyanide m-chlorophenylhydrazone selects for mutations affecting PMF-driven drug efflux pumps. *Appl. Environ. Microbiol.* 85, 1–18. doi: 10.1128/AEM.02792-18
- Gullberg, E., Albrecht, L. M., Karlsson, C., Sandegren, L., and Andersson, D. I. (2014). Selection of a multidrug resistance plasmid by sublethal levels of antibiotics and heavy metals. *MBio.* 5, 19–23. doi: 10.1128/mBio.01918-14
- Gullberg, E., Cao, S., Berg, O. G., Ilbäck, C., Sandegren, L., Hughes, D., et al. (2011). Selection of resistant bacteria at very low antibiotic concentrations. *PLoS Pathog.* 7:e1002158. doi: 10.1371/journal.ppat.1002158
- Hamdallah, I., Torok, N., Bischof, K. M., Majdalani, N., Chadalavada, S., Mdluli, N., et al. (2018). Experimental evolution of *Escherichia coli* K-12 at high pH and RpoS induction. *Appl. Environ. Microbiol.* 84:e00520. doi: 10.1128/AEM.00520-18
- Harden, M. M., He, A., Creamer, K., Clark, M. W., Hamdallah, I., Martinez, K. A., et al. (2015). Acid-adapted strains of *Escherichia coli* K-12 obtained by experimental evolution. *Appl. Environ. Microbiol.* 81, 1932–1941.
- Hasan, S. M., and Mohammadian, J. (2011). Isolation and characterization of *Halobacterium salinarum* from saline lakes in Iran. *JJM* 4, 59–65.
- He, A., Penix, S. R., Basting, P. J., Griffith, J. M., Creamer, K. E., Camperchioli, D., et al. (2017). Acid evolution of *Escherichia coli* K-12 eliminates amino acid decarboxylases and reregulates catabolism. *Appl Environ. Microbiol.* 83:e442-17. doi: 10.1128/AEM.00442-17
- Jones, D. L., and Baxter, B. K. (2017). DNA repair and photoprotection: mechanisms of overcoming environmental ultraviolet radiation exposure in halophilic archaea. *Front. Microbiol.* 8:1882. doi: 10.3389/fmicb.2017.01882
- Kanjee, U., and Houry, W. A. (2013). Mechanisms of acid resistance in *Escherichia coli*. *Annu. Rev. Microbiol.* 67, 65–81. doi: 10.1146/annurev-micro-092412-155708
- Kish, A., Kirkali, G., Robinson, C., Rosenblatt, R., Jaruga, P., Dizdaroglu, M., et al. (2009). Salt shield: intracellular salts provide cellular protection against ionizing radiation in the halophilic archaeon, *Halobacterium salinarum* NRC-1. *Environ. Microbiol.* 11, 1066–1078. doi: 10.1111/j.1462-2920.2008.01828.x
- Krulwich, T. A., Sachs, G., and Padan, E. (2011). Molecular aspects of bacterial pH sensing and homeostasis. *Nat. Rev. Microbiol.* 9, 330–343. doi: 10.1038/nrmicro2549
- Lenski, R. E., Rose, M. R., Simpson, S. C., and Tadler, S. C. (1991). Long-term experimental evolution in *Escherichia coli*. I. Adaptation and divergence during 2,000 generations. *Am. Nat.* 138, 1315–1341. doi: 10.1086/285289
- Lenski, R. E., and Travisano, M. (1994). Dynamics of adaptation and diversification: a 10,000-generation experiment with bacterial populations.

SUPPLEMENTARY MATERIAL

The Supplementary Material for this article can be found online at: <https://www.frontiersin.org/articles/10.3389/fmicb.2020.00535/full#supplementary-material>

- Proc. Natl. Acad. Sci. U.S.A. 91, 6808–6814. doi: 10.1073/pnas.91.15.6808
- Leuko, S., Domingos, C., Parpart, A., Reitz, G., and Rettberg, P. (2015). The survival and resistance of *Halobacterium salinarum* NRC-1, *Halococcus hamelinensis*, and *Halococcus morrhuae* to simulated outer space solar radiation. *Astrobiology*. 15, 987–997. doi: 10.1089/ast.2015.1310
- Lund, P., Tramonti, A., and De Biase, D. (2014). Coping with low pH: molecular strategies in neutralophilic bacteria. *FEMS Microbiol. Rev.* 38, 1091–1125. doi: 10.1111/1574-6976.12076
- Madden, M. E. E., Bodnar, R. J., and Rimstidt, J. D. (2004). Jarosite as an indicator of water-limited chemical weathering on Mars. *Nature* 431, 821–823. doi: 10.1038/nature02971
- McCarthy, S., Johnson, T., Pavlik, B. J., Payne, S., Schackwitz, W., Martin, J., et al. (2016). Expanding the limits of thermoacidophily in the archaeon *Sulfolobus solfataricus* by adaptive evolution. *Appl. Environ. Microbiol.* 82, 857–867. doi: 10.1128/AEM.03225-15
- Moore, J. P., Li, H., Engmann, M. L., Bischof, K. M., Kunka, K. S., Harris, M. E., et al. (2019). Benzoate-tolerant *Escherichia coli* strains from experimental evolution lose the Gad regulon, multi-drug efflux pumps, and hydrogenases. *Appl. Environ. Microbiol.* 85, e00966-19.
- Moran-Reyna, A., and Coker, J. A. (2014). The effects of extremes of pH on the growth and transcriptomic profiles of three haloarchaea. *F1000 Res.* 3, 1–15. doi: 10.12688/f1000research.4789.2
- Nelson-Sathi, S., Dagan, T., Landan, G., Janssen, A., Steel, M., McInerney, J. O., et al. (2012). Acquisition of 1,000 eubacterial genes physiologically transformed a methanogen at the origin of Haloarchaea. *Proc Natl Acad Sci.* 109, 20537–20542. doi: 10.1073/pnas.1209119109
- Ng, W., and DasSarma, S. (1991). “Physical and genetic mapping of the unstable gas vesicle plasmid in *Halobacterium halobium* NRC-1,” in *General and Applied Aspects of Halophilic Microorganisms*, ed. F. Rodriguez-Valera (New York NY: Plenum Press), 305–311. doi: 10.1007/978-1-4615-3730-4_37
- Ng, W. L., Arora, P., and DasSarma, S. (1993). Large deletions in class III gas vesicle-deficient mutants of *Halobacterium halobium*. *Syst. Appl. Microbiol.* 16, 560–568. doi: 10.1016/s0723-2020(11)80326-7
- Ng, W. L., Kothakota, S., and DasSarma, S. (1991). Structure of the gas vesicle plasmid in *Halobacterium halobium*: inversion isomers, inverted repeats, and insertion sequences. *J. Bacteriol.* 173, 1958–1964. doi: 10.1128/jb.173.6.1958-1964.1991
- Ng, W. V., Ciufu, S. A., Smith, T. M., Bumgarner, R. E., Baskin, D., Faust, J., et al. (1998). Snapshot of a large dynamic replicon in a halophilic archaeon: megaplasmid or minichromosome? *Genome Res.* 8, 1131–1141. doi: 10.1101/gr.8.11.1131
- Ng, W. V., Kennedy, S. P., Mahairas, G. G., Berquist, B., Pan, M., Shukla, H. D., et al. (2000). Genome sequence of *Halobacterium* species NRC-1. *Proc. Natl. Acad. Sci. U.S.A.* 97, 12176–12181. doi: 10.1073/pnas.190337797
- Oren, A. (2013). Life at high salt concentrations, intracellular KCl concentrations, and acidic proteomes. *Front. Microbiol.* 4:315.
- Pfeiffer, F., Marchfelder, A., Habermann, B., and Dyall-Smith, M. L. (2019). The genome sequence of the *Halobacterium salinarum* type strain is closely related to that of laboratory strains NRC-1 and R1. *Microbiol. Resour. Announc.* 8, e00429-19.
- Pfeiffer, F., Schuster, S. C., Broicher, A., Falb, M., Palm, P., Rodewald, K., et al. (2008). Evolution in the laboratory: the genome of *Halobacterium salinarum* strain R1 compared to that of strain NRC-1. *Genomics.* 91, 335–346. doi: 10.1016/j.ygeno.2008.01.001
- Pritchett, B. N., Elwood Madden, M. E., and Madden, A. S. (2014). Jarosite dissolution rates and maximum lifetimes in high salinity brines: implications for Earth and Mars. *Earth Planet Sci Lett.* 391, 67–68. doi: 10.1016/j.epsl.2014.01.051
- Redder, P., and Garrett, R. A. (2006). Mutations and rearrangements in the genome of *Sulfolobus solfataricus* P2. *J. Bacteriol.* 188, 4198–4206. doi: 10.1128/jb.00061-06
- Reysenbach, A., and Pace, N. R. (1995). *Archaea: A laboratory manual - Halophiles*. eds S DasSarma, M. Fleischmann, Cold Spring Harbor, NY: Cold Spring Harbor Laboratory Press.
- Robinson, J. L., Robinson, J. L., Pyzyzna, B., Pyzyzna, B., Atrasz, R. G., Atrasz, R. G., et al. (2005). Growth kinetics of extremely halophilic. *Society.* 187, 923–929. doi: 10.1128/jb.187.3.923-929.2005
- Ruepp, A., and Soppa, J. (1996). Fermentative arginine degradation in *Halobacterium salinarum* (formerly *Halobacterium halobium*): genes, gene products, and transcripts of the *arcRACB* gene cluster. *J. Bacteriol.* 178, 4942–4947. doi: 10.1128/jb.178.16.4942-4947.1996
- Sakanaka, A., Kuboniwa, M., Takeuchi, H., Hashino, E., and Amano, A. (2015). Arginine-ornithine antiporter ArcD controls arginine metabolism and interspecies biofilm development of *Streptococcus gordonii*. *J. Biol. Chem.* 290, 21185–21198. doi: 10.1074/jbc.M115.644401
- Sapienza, C., and Doolittle, W. F. (1982). Unusual physical organization of the *Halobacterium* genome. *Nature.* 295, 384–389. doi: 10.1038/295384a0
- Schou, M. F., Kristensen, T. N., Kellermann, V., Schlötterer, C., and Loeschcke, V. A. (2014). *Drosophila* laboratory evolution experiment points to low evolutionary potential under increased temperatures likely to be experienced in the future. *J. Evol. Biol.* 27, 1859–1868. doi: 10.1111/jeb.12436
- Simsek, M., DasSarma, S., RajBhandary, U., and Khorana, H. (2006). A transposable element from *Halobacterium halobium* which inactivates the bacteriorhodopsin gene. *Proc. Natl. Acad. Sci. U.S.A.* 79, 7268–7272. doi: 10.1073/pnas.79.23.7268
- Slonczewski, J. L., Fujisawa, M., Dopson, M., and Krulwich, T. A. (2009). Cytoplasmic pH measurement and homeostasis in bacteria and archaea. *Adv. Microb. Physiol.* 55, 1–79. doi: 10.1016/S0065-2911(09)05501-5
- Soppa, J. (2013). Evolutionary advantages of polyploidy in halophilic archaea. *Biochem. Soc. Trans.* 41, 339–343. doi: 10.1042/BST20120315
- Tenaillon, O., Barrick, J. E., Ribeck, N., Deatherage, D. E., Blanchard, J. L., Dasgupta, A., et al. (2016). Tempo and mode of genome evolution in a 50,000 - generation experiment. *Nature* 536, 165–170. doi: 10.1038/nature18959
- Thorvaldsdóttir, H., Robinson, J. T., Mesirov, J. P., Thorvaldsdóttir, H., Robinson, J. T., and Mesirov, J. P. (2013). Integrative genomics viewer (IGV): high-performance genomics data visualization and exploration. *Brief Bioinform.* 14, 178–192. doi: 10.1093/bib/bbs017
- Wang, G., Kennedy, S. P., Fasiludeen, S., Rensing, C., and DasSarma, S. (2004). Arsenic resistance in *Halobacterium* sp. strain NRC-1 examined by using an improved gene knockout system. *J. Bacteriol.* 186, 3187–3194. doi: 10.1128/jb.186.10.3187-3194.2004
- Wimmer, F., Oberwinkler, T., Bisle, B., Tittor, J., and Oesterhelt, D. (2008). Identification of the arginine/ornithine antiporter ArcD from *Halobacterium salinarum*. *FEBS Lett.* 582, 3771–3775. doi: 10.1016/j.febslet.2008.10.004

Conflict of Interest: The authors declare that the research was conducted in the absence of any commercial or financial relationships that could be construed as a potential conflict of interest.

Copyright © 2020 Kunka, Griffith, Holdener, Bischof, Li, DasSarma, DasSarma and Slonczewski. This is an open-access article distributed under the terms of the Creative Commons Attribution License (CC BY). The use, distribution or reproduction in other forums is permitted, provided the original author(s) and the copyright owner(s) are credited and that the original publication in this journal is cited, in accordance with accepted academic practice. No use, distribution or reproduction is permitted which does not comply with these terms.